

The substrate effect on the optical band gap of the $\text{Mg}_{0.53}\text{Zn}_{0.47}\text{O}$ thin films

S. Han^{a,b}, J.Y. Zhang^{a,*}, Z.Z. Zhang^{a,b}, Y.M. Zhao^a, D.Y. Jiang^a, Z.G. Ju^a, D.Z. Shen^a, D.X. Zhao^a, B. Yao^a

^a Key Laboratory of Excited State Processes, Changchun Institute of Optics, Fine Mechanics and Physics, Chinese Academy of Sciences, 3888 East Nan-Hu Road, Open Economic Zone, Chang Chun 130033, People's Republic of China

^b Graduate School of the Chinese Academy of Sciences, Beijing 10039, People's Republic of China

ARTICLE INFO

Article history:

Received 9 March 2010

Received in revised form 23 August 2010

Accepted 5 September 2010

PACS:

61.66.Dk

61.82.Fk

67.25.dp

Keywords:

MgZnO

Substrate

Blue shift

Rf-sputtering

ABSTRACT

MgZnO thin films were deposited on c-plane sapphire and fused quartz substrates with the same growth parameters by rf-reactive magnetron sputtering. Both the MgZnO thin films on the two substrates are single hexagonal phase and show similar Mg content. However, the absorption edge of MgZnO thin film on sapphire substrate shows a blue shift compared with that on fused quartz substrate. Similar shift also appears in the photoresponse of the detectors based on them. These phenomena were attributed to the more Mg atoms in grain boundary caused by the smaller grain size in MgZnO film on fused quartz substrate.

© 2010 Published by Elsevier B.V.

1. Introduction

Recently great interest has been concentrated on ultraviolet (UV) photodetectors due to their versatile applications, such as missile warning and tracking, engine/flame monitoring, chemical/biological agent detecting, and covert space-to-space communication [1–4]. $\text{Mg}_x\text{Zn}_{1-x}\text{O}$ is an ideal material for UV detecting because it possesses high UV absorption coefficients, high visible transparency [5–8] and large tunable band gap energy range (3.37–7.8 eV) [9–12]. Also, it is abundant, inexpensive, and environmentally friendly. Ultraviolet band (UV-B) (280–320 nm) solar radiation has a significant effect on earth's ecosystem and human health [13]. The development of reliable and low-cost UV-B monitoring devices is thus an important issue. Hexagonal $\text{Mg}_x\text{Zn}_{1-x}\text{O}$ film, with a Mg mole fraction around 0.5, is a very promising material for UV-B detection, due to its suitable band gap and superior radiation durability. Although phase separation phenomenon would exist in hexagonal $\text{Mg}_x\text{Zn}_{1-x}\text{O}$ film in this Mg content region, a lot of investigations have been made [14–19]. Recently, hexagonal $\text{Mg}_x\text{Zn}_{1-x}\text{O}$ films with Mg composition around 50% have been grown by MOCVD, MBE and rf magnetron sputtering, etc. [20–22]. Generally, Mg content is considered as the most crucial factor on the

band gap of the MgZnO, and then response cut-off edge of MgZnO detectors. However, the band gap of MgZnO is also influenced by grain size and Mg content distribution in the films. Especially for the alloy with Mg content around 50%, which is located in the thermodynamic metastable zone, the crystal quality is very sensitive to growth parameters, even substrate.

As found in this letter, difference in substrates results in the shift of the absorption edge and response peak with the same growth parameters, although the thin films still possess the same hexagonal structures and apparent Mg content of 0.53. The shift was attributed to the more interstitial Mg atoms at boundary resulted from the smaller grain size in MgZnO film on fused quartz substrate than that on sapphire.

2. Experimental

MgZnO thin films were deposited on fused quartz and c-plane sapphire substrates by rf-reactive magnetron sputtering method. High purity (99.99%) Mg target and Zn (99.99%) target were used as target materials. The sputtering chamber was pumped down to a high vacuum of 5.0×10^{-4} Pa by a turbo molecular pump. Ultra pure (5 N) Ar and O_2 gases were introduced into the sputtering chamber as the sputtering gases through a set of mass flow controllers with flow rates of 30 and 30 standard cubic centimeters per minute (SCCM), respectively. During sputtering process, the chamber pressure was kept at 2.6 Pa. The substrate temperature was kept at 600 °C. The rf powers were set as 200 W on Mg target and 100 W on Zn target, respectively. The fused quartz and sapphire substrates were placed at equivalent positions on the susceptor. The susceptor was rotated at 20 rpm to guarantee film uniformity. The thicknesses of thin films on different substrate are both about 200 nm for 2 h of growth time. Photodetectors with metal–semiconductor–metal (MSM) structure were fabricated on $\text{Mg}_x\text{Zn}_{1-x}\text{O}$ thin films using a standard photolithography tech-

* Corresponding author. Tel.: +86 43186176322; fax: +86 43185682964.
E-mail address: zhangjy53@yahoo.com.cn (J.Y. Zhang).

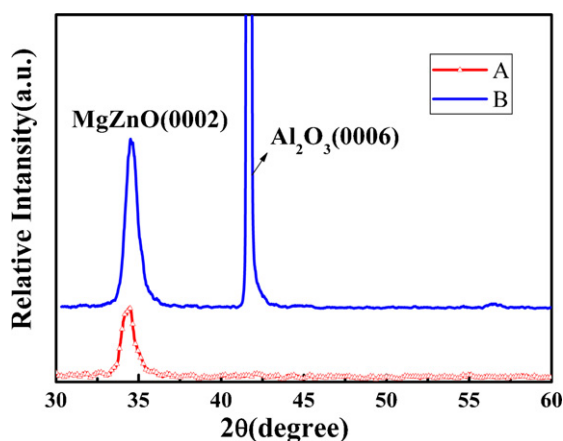


Fig. 1. XRD patterns of MgZnO films on fused quartz (curve A) and sapphire (curve B) substrates.

nique. Au was used as the electrode metal material. The electrode fingers are 5 μm wide and 500 μm long, and the spacing gap between electrode fingers is 5 μm . The structure of $\text{Mg}_x\text{Zn}_{1-x}\text{O}$ films was characterized by X-ray diffraction (XRD). Mg content was measured by Energy-dispersive X-ray Spectroscopy (EDX), the accuracy of which is 0.1%. Scanning electron microscope (SEM) was used to characterize the surface morphology and the thickness of the MgZnO thin films with uncertainty of 1–2 nm. UV–visible spectral analysis was employed to record the transmission and absorption spectra. The spectral responsivity was measured using a standard lock-in detection system with a 124A Lock-In Amplifier and a 150W Xe lamp as light source.

3. Results and discussion

Fig. 1 shows the XRD results of $\text{Mg}_{0.53}\text{Zn}_{0.47}\text{O}$ films on both substrates. Single hexagonal (0002) peak indicates the good orientation of the two $\text{Mg}_{0.53}\text{Zn}_{0.47}\text{O}$ thin films. The diffraction peak of the sample on sapphire shows larger intensity and narrower width than that on amorphous quartz substrate. Through gauss fitting, the full width at half maximum (FWHM) of the samples on sapphire and quartz are 0.7° and 0.8° , respectively. From Scherrer equation $L_{hkl} = 0.89\lambda/B \cos \theta$ [9] (L_{hkl} : size of crystal grain vertical to diffraction surface, λ : wavelength of X-ray, B : FWHM, θ : Bragg angle), the average grain size of the samples on sapphire and quartz are estimated to be 19 nm and 15 nm, respectively. **Fig. 2** shows the plots of $(ah\nu)^2$ as a function of photon energy ($h\nu$) of $\text{Mg}_x\text{Zn}_{1-x}\text{O}$ films on fused quartz and sapphire substrates. For semiconductor like MgZnO, the formula between the absorption coefficient a and

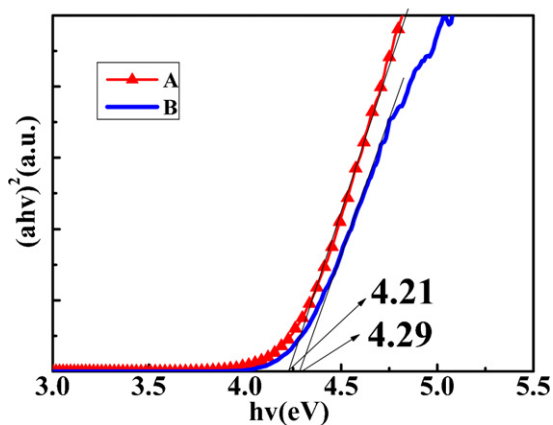


Fig. 2. Plot of $(ah\nu)^2$ as a function of photon energy ($h\nu$) of the $\text{Mg}_x\text{Zn}_{1-x}\text{O}$ thin films grown on fused quartz (curve A) and sapphire substrates (curve B). (For interpretation of the references to color in this figure legend, the reader is referred to the web version of the article.)

band gap (E_g) is $a(h\nu) = A^\#(h\nu - E_g)^{1/2}$, so from the tangent line of the plot of $(ah\nu)^2$ as a function of photon energy ($h\nu$), the band gap could be obtained from the value of $h\nu$ when $a(h\nu) = 0$. Through this method the band gaps of the two MgZnO thin films are 4.29 eV on sapphire and 4.21 eV on fused quartz. The spectral response of the MSM type UV detectors based on $\text{Mg}_x\text{Zn}_{1-x}\text{O}$ films on both the two substrates are shown in **Fig. 3(a)** and **(b)**. The responsivity of the detector was calculated by equation $R = I/P$, where R is the responsivity, I is light current and P is incident light power. For $\text{Mg}_x\text{Zn}_{1-x}\text{O}$ detector on fused quartz, the response peak locates at 283 nm with a value of 7 mA W^{-1} under 30V bias. For $\text{Mg}_x\text{Zn}_{1-x}\text{O}$ film on sapphire, the response peak locates at 270 nm with a value of 2 mA W^{-1} under 30V bias. It can be said that both the detectors exhibit good UV-B response. The peak/550 nm rejection ratios reach four and three orders of magnitude for the devices on quartz and sapphire, respectively. Here, it should be noted that the MgZnO thin film on sapphire shows a wider band gap (4.29 eV) than that on fused quartz (4.21 eV). The similar blue shift is also observed for the detectors on the two substrates. To understand the mechanism of substrate effect, Mg content, structure and surface morphology were characterized as follows.

Mg content is considered generally to be the dominant factor on the band gap of MgZnO alloys. EDX results show the Mg content in the $\text{Mg}_x\text{Zn}_{1-x}\text{O}$ films, as seen in **Fig. 4**. Mg content of $\text{Mg}_x\text{Zn}_{1-x}\text{O}$ films on sapphire and fused quartz is 53.52 and 53.76 in atom percent, respectively (**Fig. 5**). This Mg content difference between the two samples is the same with the order of random error, and is too small to bring such a large band gap difference between the two thin films.

Since the band gap shift is not supported by the EDX result, the crystal quality arises as an important factor that should be accounted in. In **Fig. 3**, although the EDX shows the similar Mg contents in the two thin films on different substrates, it cannot exclude the possibility that some Mg content concentrates at the grain boundary in the films. There are a few reports that have indicated that experimentally Mg composition is apt to concentrate on the boundary in the films [23]. In fact, the Mg contents in present MgZnO films are surely larger than that with the same band gap reported early [24]. So there would be some Mg existed in the grain boundaries in the $\text{Mg}_{0.53}\text{Zn}_{0.47}\text{O}$ thin films on both the substrates. From XRD results, no phenomenon indicates the occurrence of phase separation in the MgZnO with Mg composition over 50%, which is larger than reported value that could maintain single hexagonal structure. It also supports the possibility that a part of Mg is not in lattice. Comparing the XRD peak positions of the samples on different substrate, it can be found that the XRD peak of MgZnO film on quartz shows a small angle direction to that on sapphire, which indicates the alloy on quartz possesses larger lattice constant. It means that there are more Mg atoms at the grain boundary. In the SEM photograph of surface morphology shown in **Fig. 4**, the grain size of the $\text{Mg}_{0.53}\text{Zn}_{0.47}\text{O}$ film on quartz is significantly smaller than that on sapphire. That is to say, the boundary of the sample on quartz is denser than that on sapphire, which results in more Mg concentrating on boundary.

Moreover, it has also been widely accepted that the effects of grain boundaries plays an important role in variation of band gap (E_g). Similar study on ZnO thin films on different substrates has been discussed [25], following the treatment of Dohler [26] for compositionally modulated superlattice. The effective band gap is defined as:

$$E_g^{\text{eff}} = E_g^0 - \Phi + \xi_1, \quad (1)$$

where E_g^0 is the undistorted band gap, Φ is the barrier height at the grain boundary, and ξ_1 is the first quantized level of 1D gas. Here, from Eq. (1), more grain boundaries means narrower E_g^{eff} of

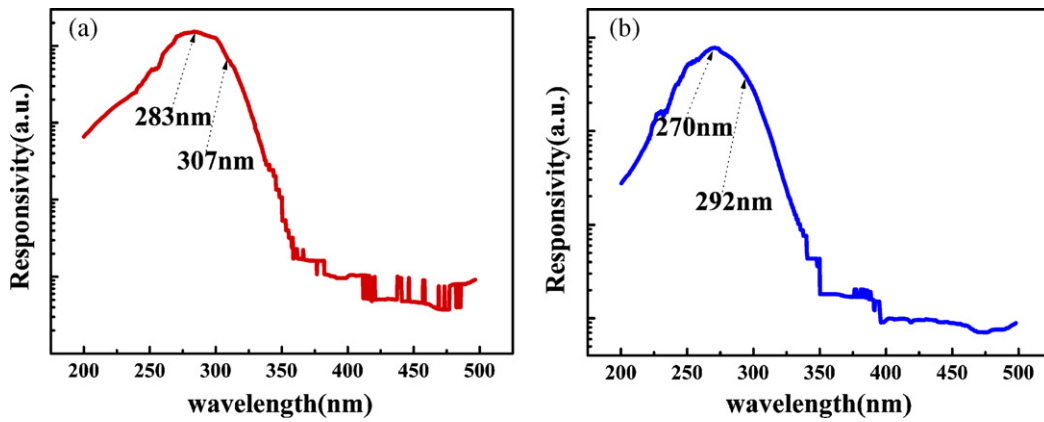


Fig. 3. Spectral response of MSM structure UV detectors based on MgZnO films on (a) fused quartz and (b) sapphire substrates.

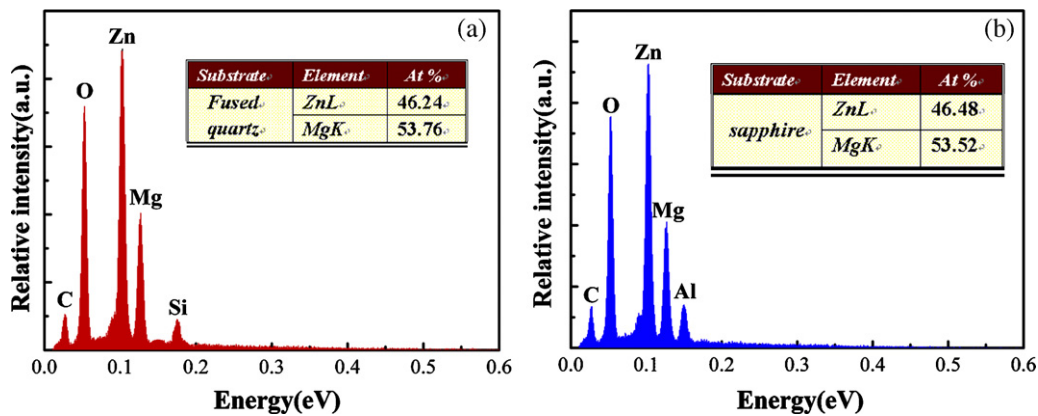


Fig. 4. EDX of MgZnO films on fused quartz (a) and c-plane sapphire (b) substrates.

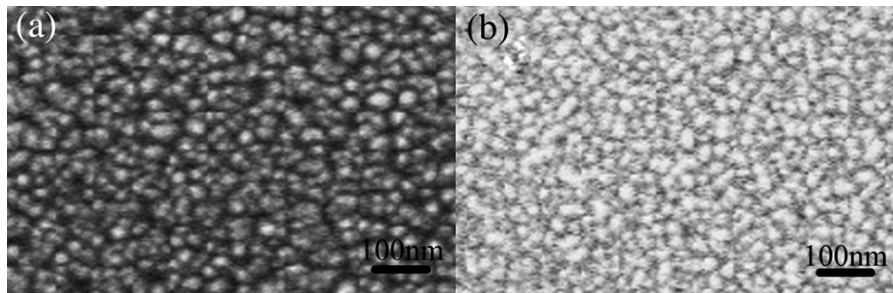


Fig. 5. SEM of MgZnO films on fused quartz (a) and sapphire (b) substrates.

Mg_xZn_{1-x}O film on quartz than that of the film on sapphire substrate. Compared with perfect single ZnO crystal, the band gap of ZnO thin film with 30–80 nm grain size on fused quartz could shift to lower energy direction for 120 meV [25]. In our case, the difference between grain sizes of Mg_{0.53}Zn_{0.47}O films on different substrate is 4 nm. Although the effect of different density of grain boundaries is not enough to bring such a big band gap shift as much as 80 meV (4.29–4.21 eV), it supported the band gap shift here.

4. Conclusion

Hexagonal Mg_{0.53}Zn_{0.47}O thin films were deposited on sapphire and fused quartz substrates by rf-reactive magnetron sputtering. Although being fabricated with the same growth parameters, the band gap of Mg_{0.53}Zn_{0.47}O film on fused quartz is smaller than that on sapphire substrate. EDX, XRD and SEM results indicate that there

is more Mg concentrates at grain boundary, which is the dominant reason for the red shift of band gap. Denser boundary in the sample on quartz than that on sapphire is also considered to answer for this decrease in band gap.

Acknowledgements

This work is supported by the “973” Program under grant nos. 2008CB317105 and 2006CB604906, the Knowledge Innovation Program of the Chinese Academy of Sciences, grant no. KJCX3.SYW.W01, and the National Natural Science Foundation of China under grant nos. 60976040 and 10974197.

References

- [1] M. Razeghi, A. Rogalski, J. Appl. Phys. 79 (1996) 7433.
- [2] M.P. Ulmer, M. Razeghi, E. Bigan, Proc. SPIE Int. 2397 (1995) 210.

- [3] A. Rogalski, M. Razeghi, *Opto-Electron. Rev.* 4 (1996) 13.
- [4] A.M. Streltsov, K.D. Moll, A.L. Gaeta, P. Kung, M.D. Walker, M. Razeghi, *Appl. Phys. Lett.* 75 (1999) 3378.
- [5] I. Takeuchi, W. Yang, K.-S. Chang, M.A. Aronova, T. Venkatesan, *J. Appl. Phys.* 94 (2003) 11.
- [6] Z.G. Ju, C.X. Shan, D.Y. Jiang, J.Y. Zhang, B. Yao, D.X. Zhao, D.Z. Shen, X.W. Fan, *Appl. Phys. Lett.* 93 (2008) 173505.
- [7] J. Chen, W.Z. Shen, N.B. Chen, D.J. Qiu, H.Z. Wu, *J. Phys. Condens. Matter* 15 (2003) L475–L482.
- [8] A. Ohtomo, M. Kawasaki, T. Koida, K. Masubuchi, H. Koinuma, *Appl. Phys. Lett.* 72 (1998) 19.
- [9] W. Yang, S.S. Hullavarad, B. Nagaraj, I. Takeuchi, R.P. Sharma, T. Venkatesan, *Appl. Phys. Lett.* 82 (2003) 3424.
- [10] H. Tanaka, S. Fujita, *Appl. Phys. Lett.* 86 (2005) 192911.
- [11] P. Yu, H.Z. Wu, T.N. Xu, D.J. Qiu, G.J. Hu, N. Dai, *J. Cryst. Growth* 310 (2008) 336–340.
- [12] A.K. Sharma, J. Narayan, J.F. Muth, C.W. Teng, C. Jin, A. Kvit, R.M. Kolbas, O.W. Holland, *Appl. Phys. Lett.* 75 (1999) 21.
- [13] A.F. McKinley, B.L. Diffey, *CIE J.* 6 (1987) 17.
- [14] J. Narayan, A.K. Sharma, A. Kvit, C. Jin, J.F. Muth, O.W. Holland, *Solid State Commun.* 121 (2002) 9.
- [15] S. Choopun, R.D. Vispute, W. Yang, R.P. Sharma, T. Venkatesan, H. Shen, *Appl. Phys. Lett.* 80 (2002) 1529.
- [16] F.D. Auret, S.A. Goodman, M. Hayes, M.J. Legodi, H.A. van Laarhoven, D.C. Look, *Appl. Phys. Lett.* 79 (2001) 3074.
- [17] W. Yang, S.S. Hullavarad, B. Nagaraj, I. Takeuchi, R.P. Sharma, T. Venkatesan, R.D. Vispute, H. Shen, *Appl. Phys. Lett.* 82 (2003) 3424.
- [18] K. Koike, K. Hamaa, I. Nakashima, G-y. Takada, K-i. Ogata, S. Sasaa, M. Inouea, M. Yano, *J. Cryst. Growth* 278 (2005) 288.
- [19] D. Jiang, C. Shan, J. Zhang, Y. Lu, B. Yao, D. Zhao, Z. Zhang, X. Fan, D. Shen, *Cryst. Growth Des.* 9 (2009) 454–456.
- [20] W.I. Park, G.-C. Yi, H.M. Jang, *Appl. Phys. Lett.* 79 (2001) 2022.
- [21] Z.L. Liu, Z.X. Mei, T.C. Zhang, Y.P. Liu, Y. Guo, X.L. Du, A. Hallen, J.J. Zhu, A.Y. Kuznetsov, *J. Cryst. Growth* 311 (2009) 4356–4359.
- [22] C.X. Cong, B. Yao, S.Z. Xing, Y.P. Xie, L.X. Guan, B.H. Li, X.H. Wang, Z.P. Wei, Z.Z. Zhang, Y.M. Lu, D.Z. Shen, X.W. Fan, *Appl. Phys. Lett.* 89 (2006) 262108.
- [23] I. Takeuchi, W. Yang, K.S. Chang, M.A. Aronova, T. Venkatesan, R.D. Vispute, L.A. Bendersky, *J. Appl. Phys.* 94 (2003) 7336.
- [24] D. Jiang, C. Shan, J. Zhang, Y. Lu, B. Yao, D. Zhao, Z. Zhang, X. Fan, D. Shen, *Cryst. Growth Des.* 9 (1) (2009) 454–456.
- [25] V. Srikant, D.R. Clarke, *J. Appl. Phys.* 81 (1997) 9.
- [26] G.H. Dohler, *IEEE J. Quantum Electron.* 22 (1986) 1682.